

# Nonreciprocal transition with cyclic four-level transition

Xun-Wei Xu,<sup>1,2,\*</sup> Hai-Quan Shi,<sup>2</sup> and Ai-Xi Chen<sup>3,2,†</sup>

<sup>1</sup>*Key Laboratory of Low-Dimensional Quantum Structures and Quantum Control of Ministry of Education, Department of Physics and Synergetic Innovation Center for Quantum Effects and Applications, Hunan Normal University, Changsha 410081, China*

<sup>2</sup>*Department of Applied Physics, East China Jiaotong University, Nanchang, 330013, China*

<sup>3</sup>*Department of Physics, Zhejiang Sci-Tech University, Hangzhou 310018, China*

(Dated: December 22, 2024)

We propose a theoretical scheme to realize nonreciprocal transition in a multi-level atomic system with cyclic four-level transition. The effective transition between two indirectly coupled energy levels become nonreciprocal, when they are coupled to two auxiliary levels simultaneously, by four strong driving fields with the total phase serving as a synthetic magnetic flux and breaking the time reversal symmetry of the system. The nonreciprocal transition can lead to the elimination of a spectral line in the spontaneous emission spectrum, which provide us a simple approach to measure the phenomenon in steady state. This work provides a feasible approach to observe nonreciprocal transition in a wide range of multi-level systems, including natural atoms with parity symmetry.

## I. INTRODUCTION

Time reversal symmetry is the hypothesis that certain physical quantities are unchanged under time reversal transformation, which is related to reversibility of the system, such as the principle of detailed balancing in kinetic systems [1]. With the principle of detailed balance as a background, A. Einstein proposed his quantum theory of radiation [2] in 1916, which is now considered as the theoretical foundation of the laser, and one of the important corollaries is the absorption coefficient should be equal to the stimulated emission coefficient between two nondegenerate energy levels. However, sometimes we need to break the time reversal symmetry of atomic systems to yield fantastic phenomena, e.g., cyclic population transfer [3], controllable electromagnetically induced transparency [4], gain without inversion [5].

One important approach to break the time reversal symmetry of atomic systems is based on the cyclic three-level transitions in the superconducting qubit circuit with three Josephson junctions [6, 7], and chiral molecules [3, 8, 9]. The cyclic three-level transitions in multi-level atomic systems have been used to generate many interesting phenomena in single-photon level, including single-photon quantum routing [10], single-photon second-order nonlinear processes [11–13]. When the three passible transitions in the cyclic three-level structure are driven by three mutually phase-locked driving fields, the time reversal symmetry of atomic system can be broken by the magnetic flux synthesized from the driving-field phase. In a recent experiment, time-reversal symmetry breaking and cyclic population transfer were revealed in a single nitrogen-vacancy spin system by controlling the global phase of the driving fields [14].

On the basis above, a multi-level atomic system with

cyclic three-level transition was proposed to realize significant difference between the stimulated emission and absorption coefficients of two nondegenerate energy levels, which was referred to as nonreciprocal transition [15]. Different from the closed-contour spin dynamics [14], besides synthetic magnetism, reservoir engineering was also employed to eliminate one of the transitions in opposite directions [15]. It was shown that the nonreciprocal transition can lead to the elimination of a spectral line in the spontaneous emission spectrum [16]. The multi-level atomic systems with nonreciprocal transition has a potential application for nonreciprocal photon/phonon devices design [15, 17, 18] and molecular detection [16]. However, the cyclic three-level transition only occur in the atomic systems broken parity symmetry, which can not be observed in natural atoms due to the rules of electric dipole transitions in general. How to observe nonreciprocal transition in in atomic systems with parity symmetry, e.g., natural atoms, is still an open question.

In this paper, we investigate the transitions in a multi-level atomic system with cyclic four-level transition, which can be realized under the rules of electric dipole transitions. In the cyclic four-level transition model, we show that two energy levels without direct transition can exhibit nonreciprocal transition, with two other energy levels as auxiliary levels coupled to them simultaneously with four strong driving fields. The total phase of the four strong driving fields around the cyclic four-level transition serves as a synthetic magnetic flux through the four levels and breaks the time reversal symmetry of the system, which is the physical fundamental for nonreciprocal transitions. It's important to note that, different from the model with cyclic three-level transition in Refs. [15, 16], here the cyclic four-level transition can be implemented in the natural atoms without breaking the parity symmetry of the system. Moreover, there is not any strict restriction on the energy difference between the two energy levels for nonreciprocal transition, so that nonreciprocal transition based on cyclic four-level transition can be realized between two degenerate energy levels.

\* davidxu0816@163.com

† aixichen@zstu.edu.cn

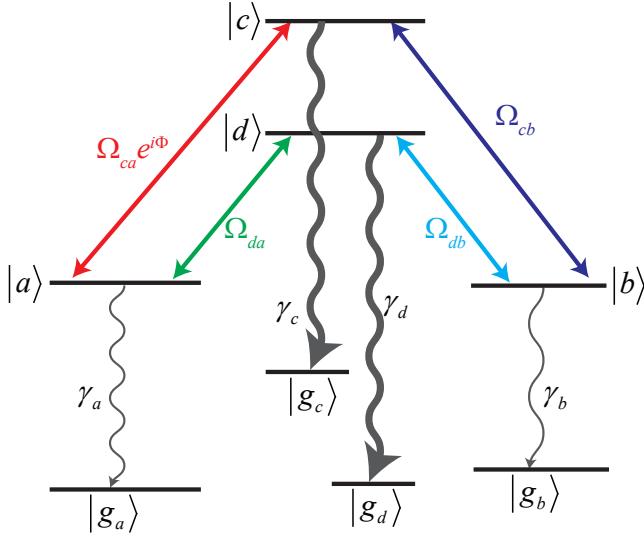


FIG. 1. (Color online) Level diagram of an atom or molecule with cyclic transitions for the four upper levels ( $|a\rangle$ ,  $|b\rangle$ ,  $|c\rangle$ , and  $|d\rangle$ ), and they are coupled by the same vacuum modes to different lower levels ( $|g_a\rangle$ ,  $|g_b\rangle$ ,  $|g_c\rangle$ , and  $|g_d\rangle$ ).

The remainder of this paper is organized as follows. In Sec. II, a multi-level system is introduced and the dynamical equations are given under the Weisskopf-Wigner approximation. The time evolution of the populations

and the transition probabilities between two levels are investigated, and nonreciprocal transitions are shown in Sec. III. Moreover, the spontaneous emission spectra of the systems with nonreciprocal transitions are discussed in Sec. IV, which provide us a convenient way to measure nonreciprocal transitions in experiments. Finally, the conclusions is given in Sec. V.

## II. HAMILTONIAN AND DYNAMICAL EQUATIONS

We study the spontaneous emission of an atom or molecule with four upper levels ( $|a\rangle$ ,  $|b\rangle$ ,  $|c\rangle$ , and  $|d\rangle$ ), which are coupled to each other by four strong fields with frequencies ( $\nu_{ca}$ ,  $\nu_{cb}$ ,  $\nu_{db}$ , and  $\nu_{da}$ ), Rabi frequencies ( $\Omega_{ca}$ ,  $\Omega_{cb}$ ,  $\Omega_{db}$ , and  $\Omega_{da}$ ) and phases ( $\phi_{ca}$ ,  $\phi_{cb}$ ,  $\phi_{db}$ , and  $\phi_{da}$ ). For different systems, the upper levels may be coupled to the same lower level or to different lower levels respectively, where the spontaneous emission from multiple upper levels to the common lower level may result in spontaneous emission cancellation and spectral line elimination [19, 20], which is not the focus of this paper. In order to eliminate this effect, the spontaneous emission spectrum for the system will be derived for the case that the four upper levels are coupled to four different lower levels ( $|g_a\rangle$ ,  $|g_b\rangle$ ,  $|g_c\rangle$ , and  $|g_d\rangle$ ) respectively with the same vacuum modes, as shown in Fig. 1. The Hamiltonian is given by ( $\hbar = 1$ )

$$\begin{aligned}
 H = & \Omega_{ca} e^{i\Phi} e^{-i\Delta_{ca}t} |a\rangle \langle c| + \Omega_{cb} e^{i\Delta_{cb}t} |c\rangle \langle b| + \Omega_{da} e^{i\Delta_{da}t} |d\rangle \langle a| + \Omega_{db} e^{-i\Delta_{db}t} |b\rangle \langle d| \\
 & + \sum_k \left[ g_k^a e^{i(\omega_{ag} - \omega_k)t} v_k |a\rangle \langle g_a| + g_k^b e^{i(\omega_{bg} - \omega_k)t} v_k |b\rangle \langle g_b| + g_k^c e^{i(\omega_{cg} - \omega_k)t} v_k |c\rangle \langle g_c| + g_k^d e^{i(\omega_{dg} - \omega_k)t} v_k |d\rangle \langle g_d| \right] \\
 & + \text{H.c.},
 \end{aligned} \tag{1}$$

where  $v_k$  ( $v_k^\dagger$ ) is the annihilation (creation) operator for the  $k$ th vacuum mode with frequency  $\omega_k$ ,  $\omega_{ij}$  (or  $\omega_{ig}$ ) is the frequency difference between levels  $|i\rangle$  and  $|j\rangle$  (or  $|g_i\rangle$ ) with ( $i, j = a, b, c, d$ ),  $\Delta_{ij} \equiv \omega_{ij} - \nu_{ij}$  is the detuning of the driving fields, and  $g_k^i$  is the coupling constant between the  $k$ th vacuum mode and the atomic transition from  $|i\rangle$  to  $|g_i\rangle$ . Here  $k$  denotes both the momentum and polarization of the vacuum modes, and  $\Phi \equiv \phi_{ca} + \phi_{db} + \phi_{cb} + \phi_{da}$  is the total phase of the four strong driving fields through the cycle-transition  $|a\rangle \rightarrow |d\rangle \rightarrow |b\rangle \rightarrow |c\rangle \rightarrow |a\rangle$ . As the phase of the coupling constant  $g_k^i$  does not matter in the following discussions, real  $g_k^i$  is assumed for notational convenience. For simplicity, we also make the assumption of resonance  $\Delta_c \equiv \Delta_{ac} = \Delta_{bc}$  and  $\Delta_d \equiv \Delta_{da} = \Delta_{db}$ .

In this paper, we will focus on the nonreciprocal transition between levels  $|a\rangle$  and  $|b\rangle$ . To investigate the transition probabilities between the upper levels  $|a\rangle$  and  $|b\rangle$ , we assume that the system is initially prepared in one of them, i.e.,  $|\psi(0)\rangle = |a\rangle|0\rangle$  or  $|\psi(0)\rangle = |b\rangle|0\rangle$ , where  $|0\rangle$  denotes the vacuum state. The state vector for this system at time  $t$  can be written as

$$|\psi(t)\rangle = [A(t)|a\rangle + B(t)|b\rangle + C(t)|c\rangle + D(t)|d\rangle]|0\rangle + \sum_{i=a,b,c,d} \sum_k G_k^i(t) v_k^\dagger |g_i\rangle |0\rangle, \tag{2}$$

where the modulus squares of the coefficients  $A(t)$ ,  $B(t)$ ,  $C(t)$ ,  $D(t)$ , and  $G_k^i(t)$  are the occupation probabilities in the corresponding state at time  $t$ . By using the Weisskopf-Wigner approximation [21, 22], the dynamical behaviors for the coefficients are obtained from the Schrödinger equation  $d|\psi(t)\rangle/dt = -iH|\psi(t)\rangle$  as

$$\frac{d}{dt} A(t) = -\frac{\gamma_a}{2} A(t) - i\Omega_{ca} e^{i\Phi} e^{-i\Delta_{ca}t} C(t) - i\Omega_{da} e^{-i\Delta_{da}t} D(t), \tag{3}$$

$$\frac{d}{dt}B(t) = -\frac{\gamma_b}{2}B(t) - i\Omega_{cb}e^{-i\Delta_c t}C(t) - i\Omega_{db}e^{-i\Delta_d t}D(t), \quad (4)$$

$$\frac{d}{dt}C(t) = -\frac{\gamma_c}{2}C(t) - i\Omega_{ca}e^{-i\Phi}e^{i\Delta_c t}A(t) - i\Omega_{cb}e^{i\Delta_c t}B(t), \quad (5)$$

$$\frac{d}{dt}D(t) = -\frac{\gamma_d}{2}D(t) - i\Omega_{da}e^{i\Delta_d t}A(t) - i\Omega_{db}e^{i\Delta_d t}B(t), \quad (6)$$

$$\frac{d}{dt}G_k^a(t) = -ig_k^a e^{-i(\omega_{ag}-\omega_k)t}A(t), \quad (7)$$

$$\frac{d}{dt}G_k^b(t) = -ig_k^b e^{-i(\omega_{bg}-\omega_k)t}B(t), \quad (8)$$

$$\frac{d}{dt}G_k^c(t) = -ig_k^c e^{-i(\omega_{cg}-\omega_k)t}C(t), \quad (9)$$

$$\frac{d}{dt}G_k^d(t) = -ig_k^d e^{-i(\omega_{dg}-\omega_k)t}D(t), \quad (10)$$

where  $\gamma_a = [2\pi(g_k^a)^2\rho(\omega_k)]_{\omega_k=\omega_{ag}}$ ,  $\gamma_b = [2\pi(g_k^b)^2\rho(\omega_k)]_{\omega_k=\omega_{bg}}$ ,  $\gamma_c = [2\pi(g_k^c)^2\rho(\omega_k)]_{\omega_k=\omega_{cg}}$ , and  $\gamma_d = [2\pi(g_k^d)^2\rho(\omega_k)]_{\omega_k=\omega_{dg}}$  are the decay rates from the four upper levels, and  $\rho(\omega_k)$  is the mode density around the system. For convenience of calculations, let us define  $\tilde{C}(t) \equiv e^{-i\Delta_c t}C(t)$ ,  $\tilde{D}(t) \equiv e^{-i\Delta_d t}D(t)$ , then the dynamical equations (3)-(6) can be rewritten with constant coefficients as

$$\frac{d}{dt}A(t) = -\frac{\gamma_a}{2}A(t) - i\Omega_{ca}e^{i\Phi}\tilde{C}(t) - i\Omega_{da}\tilde{D}(t), \quad (11)$$

$$\frac{d}{dt}B(t) = -\frac{\gamma_b}{2}B(t) - i\Omega_{cb}\tilde{C}(t) - i\Omega_{db}\tilde{D}(t), \quad (12)$$

$$\frac{d}{dt}\tilde{C}(t) = \left(-i\Delta_c - \frac{\gamma_c}{2}\right)\tilde{C}(t) - i\Omega_{ca}e^{-i\Phi}A(t) - i\Omega_{cb}B(t), \quad (13)$$

$$\frac{d}{dt}\tilde{D}(t) = \left(-i\Delta_d - \frac{\gamma_d}{2}\right)\tilde{D}(t) - i\Omega_{da}A(t) - i\Omega_{db}B(t). \quad (14)$$

### III. TRANSITION PROBABILITIES

The dynamic Eqs. (11)-(14) can be concisely expressed as

$$i\frac{d\Psi(t)}{dt} = H_{\text{eff}}\Psi(t), \quad (15)$$

where  $\Psi(t) = [A(t), B(t), \tilde{C}(t), \tilde{D}(t)]^T$ , and

$$H_{\text{eff}} = \begin{pmatrix} -i\frac{\gamma_a}{2} & 0 & \Omega_{ca}e^{i\Phi} & \Omega_{da} \\ 0 & -i\frac{\gamma_b}{2} & \Omega_{cb} & \Omega_{db} \\ \Omega_{ca}e^{-i\Phi} & \Omega_{cb} & \Delta_c - i\frac{\gamma_c}{2} & 0 \\ \Omega_{da} & \Omega_{db} & 0 & \Delta_d - i\frac{\gamma_d}{2} \end{pmatrix}. \quad (16)$$

The general solution of Eq. (15) can be written as

$$\Psi(t) = U(t)\Psi(0), \quad (17)$$

with the initial conditions  $\Psi(0) = [A(0), B(0), C(0), D(0)]^T$ , and the time-evolution matrix

$$U(t) \equiv e^{-iH_{\text{eff}}t}. \quad (18)$$

The transition probabilities from  $|a\rangle$  to  $|b\rangle$  [ $T_{ba}(t)$ ] and from  $|b\rangle$  to  $|a\rangle$  [ $T_{ab}(t)$ ] are defined as

$$T_{ba}(t) \equiv |U_{21}(t)|^2, \quad (19)$$

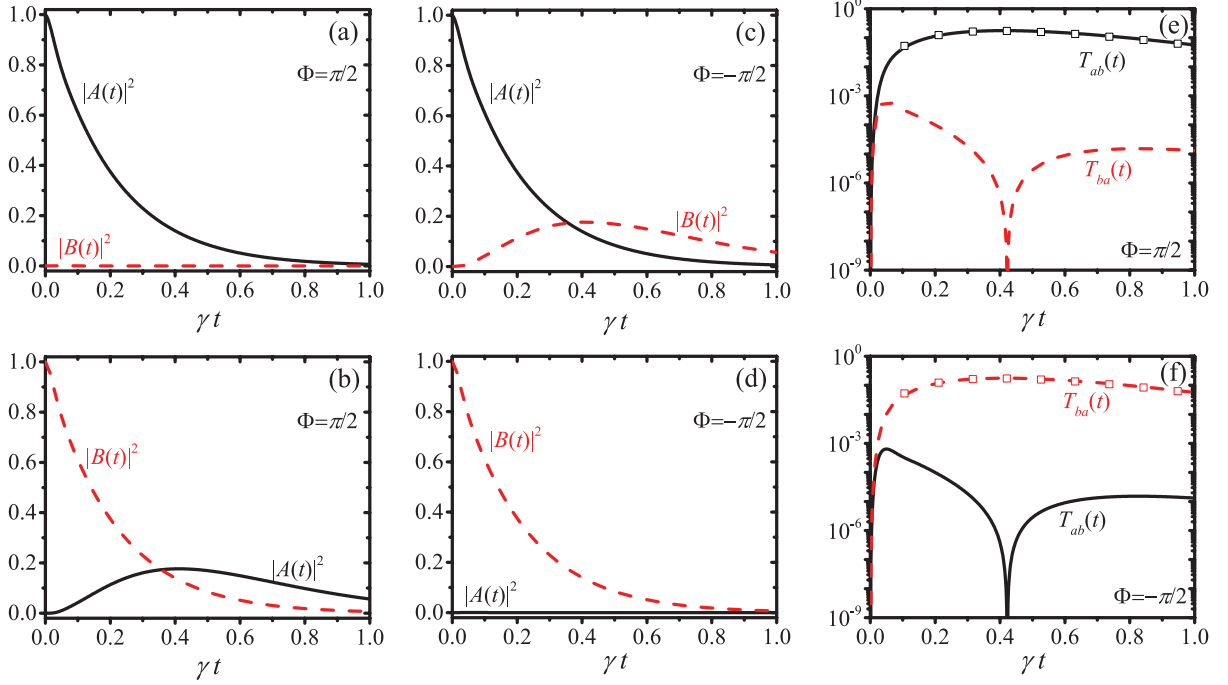


FIG. 2. (Color online) The populations  $|A(t)|^2$  (black solid curve) and  $|B(t)|^2$  (red dashed curve) are plotted as functions of the time  $\gamma t$  for:  $\Phi = \pi/2$  in (a) and (b);  $\Phi = -\pi/2$  in (c) and (d). The initial conditions are  $A(0) = 1$  and  $B(0) = C(0) = D(0) = 0$  for (a) and (c),  $B(0) = 1$  and  $A(0) = C(0) = D(0) = 0$  for (b) and (d). The transition probabilities  $T_{ab}(t)$  (black solid curve) and  $T_{ba}(t)$  (red dashed curve) are plotted as functions of the time  $\gamma t$  for: (e)  $\Phi = \pi/2$ ; (f)  $\Phi = -\pi/2$ . The other parameters are  $\gamma_a = \gamma_b = \gamma$ ,  $\gamma_c = \gamma_d = 100\gamma$ ,  $\Omega_{ca} = \Omega_{cb} = \Omega_{da} = \Omega_{db} = 10\gamma$ ,  $\Delta_c = -\Delta_d = 50\gamma$ .

$$T_{ab}(t) \equiv |U_{12}(t)|^2, \quad (20)$$

where  $U_{ij}(t)$  (for  $i, j = 1, 2, 3, 4$ ) represents the element at the  $i$ th row and  $j$ th column of the matrix  $U(t)$  given by Eq. (18). Moreover, the isolation for the nonreciprocal transition between levels  $|a\rangle$  and  $|b\rangle$  is defined by

$$I(t) \equiv \frac{T_{ab}(t)}{T_{ba}(t)}. \quad (21)$$

Here, we assume that the decay rates of the upper levels  $|c\rangle$  and  $|d\rangle$  are much larger than the other parameters, i.e.,  $\min\{\gamma_c, \gamma_d\} \gg \max\{\gamma_a, \gamma_b, \Omega_{ca}, \Omega_{cb}, \Omega_{da}, \Omega_{db}\}$ . From Eqs. (13) and (14) by adiabatic approximation, we have

$$\tilde{C}(t) = -\frac{i\Omega_{ca}}{i\Delta_c + \frac{\gamma_c}{2}} e^{-i\Phi} A(t) - \frac{i\Omega_{cb}}{i\Delta_c + \frac{\gamma_c}{2}} B(t), \quad (22)$$

$$\tilde{D}(t) = \frac{-i\Omega_{da}}{i\Delta_d + \frac{\gamma_d}{2}} A(t) + \frac{-i\Omega_{db}}{i\Delta_d + \frac{\gamma_d}{2}} B(t). \quad (23)$$

Substitute these into Eqs. (11) and (12), the effective dynamic equations can be written as

$$\frac{d}{dt} A(t) = -\left(\frac{\gamma_{a,\text{eff}}}{2} + i\Delta_{a,\text{eff}}\right) A(t) - J_{ab} B(t), \quad (24)$$

$$\frac{d}{dt} B(t) = -\left(\frac{\gamma_{b,\text{eff}}}{2} + i\Delta_{b,\text{eff}}\right) B(t) - J_{ba} A(t) \quad (25)$$

with effective decay rates, detunings

$$\gamma_{a,\text{eff}} = \gamma_a + \frac{4\gamma_c\Omega_{ca}^2}{4\Delta_c^2 + \gamma_c^2} + \frac{4\gamma_d\Omega_{da}^2}{4\Delta_d^2 + \gamma_d^2}, \quad (26)$$

$$\gamma_{b,\text{eff}} = \gamma_b + \frac{4\gamma_c\Omega_{cb}^2}{4\Delta_c^2 + \gamma_c^2} + \frac{4\gamma_d\Omega_{db}^2}{4\Delta_d^2 + \gamma_d^2}, \quad (27)$$

$$\Delta_{a,\text{eff}} = -\frac{4\Delta_c\Omega_{ca}^2}{4\Delta_c^2 + \gamma_c^2} - \frac{4\Delta_d\Omega_{da}^2}{4\Delta_d^2 + \gamma_d^2}, \quad (28)$$

$$\Delta_{b,\text{eff}} = -\frac{4\Delta_c\Omega_{cb}^2}{4\Delta_c^2 + \gamma_c^2} - \frac{4\Delta_d\Omega_{db}^2}{4\Delta_d^2 + \gamma_d^2}, \quad (29)$$

and effective coupling coefficients

$$J_{ab} = \frac{\Omega_{ca}\Omega_{cb}e^{i\Phi}}{i\Delta_c + \frac{\gamma_c}{2}} + \frac{\Omega_{da}\Omega_{db}}{i\Delta_d + \frac{\gamma_d}{2}}, \quad (30)$$

$$J_{ba} = \frac{\Omega_{ca}\Omega_{cb}e^{-i\Phi}}{i\Delta_c + \frac{\gamma_c}{2}} + \frac{\Omega_{da}\Omega_{db}}{i\Delta_d + \frac{\gamma_d}{2}}. \quad (31)$$

The condition for nonreciprocal transition is  $J_{ab} \neq J_{ba}$ , i.e.,  $\Phi \neq n\pi$  ( $n$  is an integer). This can be understood intuitively that  $\Phi \neq n\pi$  breaks the time-reversal symmetry of the Hamiltonian given in Eq. (1).

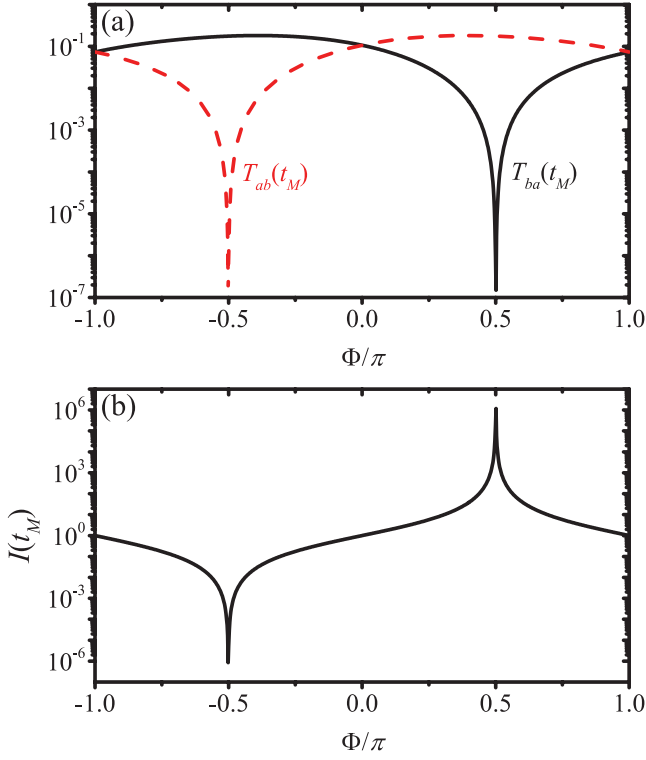


FIG. 3. (Color online) (a) The transition probabilities  $T_{ba}(t)$  and  $T_{ab}(t)$ , and (b) the isolation  $I(t)$  are plotted as functions of the synthetic magnetic flux  $\Phi$  at time  $t = t_M$ . The other parameters are the same as in Fig. 2.

One necessary condition for optimal nonreciprocal transition is one of the effective coupling coefficients ( $J_{ab}$  or  $J_{ba}$ ) equal zero, i.e.,

$$e^{\pm i\Phi} = -\frac{(i2\Delta_c + \gamma_c) \Omega_{da}\Omega_{db}}{(i2\Delta_d + \gamma_d) \Omega_{ca}\Omega_{cb}}. \quad (32)$$

The transition probabilities from  $|a\rangle$  to  $|b\rangle$  [ $T_{ba}(t)$ ] and from  $|b\rangle$  to  $|a\rangle$  [ $T_{ab}(t)$ ] can be obtained approximately under this condition. For simplicity, we choose the symmetric parameters:  $\Omega_{ca} = \Omega_{cb} = \Omega_{da} = \Omega_{db}$ ,  $\gamma_a = \gamma_b$ ,  $\gamma_c = \gamma_d$ ,  $\Delta_c = -\Delta_d$ . The condition  $J_{ab} = 0$  ( $J_{ba} = 0$ ) is satisfied for  $\Phi = -\pi/2$  ( $\Phi = \pi/2$ ) with detuning  $\Delta_c = -\Delta_d = \gamma_c/2 = \gamma_d/2$ , and we have transition probabilities

$$T_{ba}(t) \approx \left| J_{ba} t \exp \left[ - \left( \frac{\gamma_{b,\text{eff}}}{2} + i\Delta_{b,\text{eff}} \right) t \right] \right|^2, \quad (33)$$

for initial conditions  $A(0) = 1$  and  $B(0) = C(0) = D(0) = 0$ , and

$$T_{ab}(t) \approx \left| J_{ab} t \exp \left[ - \left( \frac{\gamma_{a,\text{eff}}}{2} + i\Delta_{a,\text{eff}} \right) t \right] \right|^2 \quad (34)$$

for initial conditions  $B(0) = 1$  and  $A(0) = C(0) = D(0) = 0$ . The transition probabilities are time dependent, and the time for maximal transition probability is

$$t_M \approx \frac{2}{\gamma_{b,\text{eff}}} = \frac{2}{\gamma_{a,\text{eff}}}, \quad (35)$$

with transition probabilities

$$T_{ba}(t_M) \approx \left| \frac{2 J_{ba}}{e \gamma_{b,\text{eff}}} \right|^2, \quad (36)$$

$$T_{ab}(t_M) \approx \left| \frac{2 J_{ab}}{e \gamma_{a,\text{eff}}} \right|^2, \quad (37)$$

where  $e$  is the mathematical constant approximately equal to 2.71828.

The populations  $|A(t)|^2$  (black solid curve) and  $|B(t)|^2$  (red dashed curve) obtained from Eqs. (16)-(18) are plotted as functions of the time  $t$  in Figs. 2(a)-2(d). It is clear that the population can transfer from the level  $|b\rangle$  to level  $|a\rangle$  for  $\Phi = \pi/2$ , but almost no population will transfer from the level  $|a\rangle$  to level  $|b\rangle$ . In contrast, the population can transfer from the level  $|a\rangle$  to level  $|b\rangle$ , but almost no population will transfer from the level  $|b\rangle$  to level  $|a\rangle$  when  $\Phi = -\pi/2$ .

The transition probabilities from  $|b\rangle$  to  $|a\rangle$  [ $T_{ab}(t)$ ] and from  $|a\rangle$  to  $|b\rangle$  [ $T_{ba}(t)$ ] can also be obtained from Eqs. (18)-(20). They are plotted as functions of time  $t$  in Figs. 2(e) and 2(f). It is clear that  $T_{ab}(t) \gg T_{ba}(t)$  for  $\phi = \pi/2$ , and  $T_{ab}(t) \ll T_{ba}(t)$  for  $\phi = -\pi/2$ , i.e., the transitions between levels  $|b\rangle$  and  $|a\rangle$  are nonreciprocal. The approximate analytical results given in Eqs. (33) and (34) are shown by open squares in Figs. 2(e) and 2(f), which agree well with the solid and dashed curves obtained from Eqs. (18)-(20).

Furthermore, the dependence of the transition probabilities  $T_{ba}(t)$  and  $T_{ab}(t)$  on the synthetic magnetic flux  $\Phi$  is shown in Fig. 3(a). At time  $t = t_M$ , we have  $T_{ba}(t) < T_{ab}(t)$  for synthetic magnetic flux  $0 < \Phi < \pi$ ; in the contrast, we have  $T_{ba}(t) > T_{ab}(t)$  for synthetic magnetic flux  $-\pi < \Phi < 0$ . As shown in Fig. 3(b), under the conditions  $\Omega_{ca} = \Omega_{cb} = \Omega_{da} = \Omega_{db}$  and  $\Delta_c = -\Delta_d = \gamma_c/2 = \gamma_d/2$ , the optimal isolation  $I(t)$  is obtained with synthetic magnetic flux  $\Phi = \pm\pi/2$ .

#### IV. SPONTANEOUS EMISSION SPECTRUM

To measure the nonreciprocal transitions in the steady states, we need other ingredient in the system, i.e., the decay rates of upper levels, which play a key role in suppressing the transition probabilities in one direction but not the other. The nonreciprocal transitions can be observed by measuring the spontaneous emission spectra of the system. In the following, we will use the Laplace transform method to obtain the spontaneous emission spectra of the system. By taking the Laplace transform, i.e.,  $\bar{O}(s) = \int_0^{+\infty} O(t) e^{-st} dt$ , of Eqs. (11)-(14), with the initial condition  $\Psi(0) = [A(0), B(0), C(0), D(0)]^T$ , we get [19, 20]

$$\bar{\Psi}(s) = M^{-1} \Psi(0) \quad (38)$$

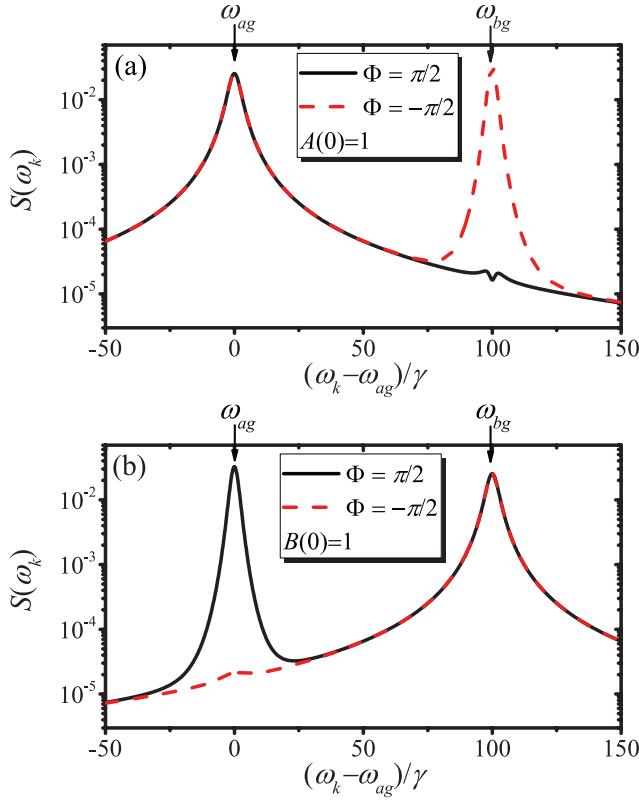


FIG. 4. (Color online) The spontaneous emission spectrum  $S(\omega_k)$  is plotted as a function of the detuning  $(\omega_k - \omega_{ag})/\gamma$  for synthetic magnetic flux  $\Phi = \pi/2$  (black solid curve) and  $\Phi = -\pi/2$  (red dashed curve), with initial conditions  $A(0) = 1$  and  $B(0) = C(0) = D(0) = 0$  in (a), and  $B(0) = 1$  and  $A(0) = C(0) = D(0) = 0$  in (b). In both (a) and (b), we set  $\omega_{bg} - \omega_{ag} = 100\gamma$ ,  $\omega_{cg} - \omega_{ag} = 1000\gamma$ , and  $\omega_{dg} - \omega_{ag} = 2000\gamma$ . The other parameters are the same as in Fig. 2.

with  $\overline{\Psi}(s) = [\overline{A}(s), \overline{B}(s), \overline{C}(s), \overline{D}(s)]^\top$ , and

$$M = \begin{pmatrix} s + \frac{\gamma_a}{2} & 0 & i\Omega_{ca}e^{i\Phi} & i\Omega_{da} \\ 0 & s + \frac{\gamma_b}{2} & i\Omega_{cb} & i\Omega_{db} \\ i\Omega_{ca}e^{-i\Phi} & i\Omega_{cb} & s + \frac{\gamma_c}{2} + i\Delta_c & 0 \\ i\Omega_{da} & i\Omega_{db} & 0 & s + \frac{\gamma_d}{2} + i\Delta_d \end{pmatrix}. \quad (39)$$

The spontaneous emission spectrum of the system [19, 20],  $S(\omega)$ , is the Fourier transform of

$$\begin{aligned} & \langle E^-(t+\tau) E^+(t) \rangle_{t \rightarrow +\infty} \\ & \equiv \langle \psi(t) | \sum_{k,k'} v_k^\dagger e^{i\omega_k(t+\tau)} v_{k'} e^{-i\omega_{k'}t} | \psi(t) \rangle_{t \rightarrow +\infty} \\ & = \int_{-\infty}^{+\infty} \sum_{i=a,b,c,d} |G_k^i(t)|_{t \rightarrow +\infty}^2 \rho(\omega_k) e^{i\omega_k \tau} d\omega_k, \quad (40) \end{aligned}$$

then we have  $S(\omega_k) = \sum_{i=a,b,c,d} |G_k^i(+\infty)|^2 \rho(\omega_k)$ , where  $G_k^i(+\infty) \equiv G_k^i(t)|_{t \rightarrow +\infty}$  is the long time behavior ( $t \rightarrow +\infty$ ) of  $G_k^i(t)$  and can be obtained by integrating

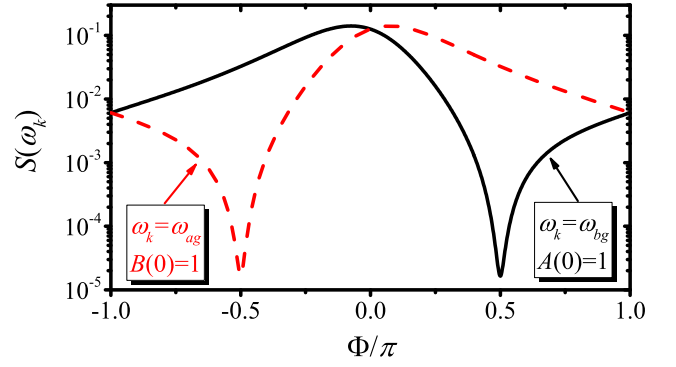


FIG. 5. (Color online) The spontaneous emission spectrum  $S(\omega_k)$  is plotted as a function of the synthetic magnetic flux  $\Phi$ : (black solid curve) with frequency  $\omega_k = \omega_{bg}$  and initial conditions  $A(0) = 1$  and  $B(0) = C(0) = D(0) = 0$ , and (red dashed curve) with frequency  $\omega_k = \omega_{ag}$  and initial conditions  $B(0) = 1$  and  $A(0) = C(0) = D(0) = 0$ . The other parameters are the same as in Fig. 4.

time  $t$  in Eqs. (7)-(10) as

$$G_k^a(+\infty) = -ig_k^a \overline{A}[i(\omega_{ag} - \omega_k)], \quad (41)$$

$$G_k^b(+\infty) = -ig_k^b \overline{B}[i(\omega_{bg} - \omega_k)], \quad (42)$$

$$G_k^c(+\infty) = -ig_k^c \overline{C}[i(\omega_{cg} - \Delta_c - \omega_k)], \quad (43)$$

$$G_k^d(+\infty) = -ig_k^d \overline{D}[i(\omega_{dg} - \Delta_d - \omega_k)]. \quad (44)$$

Thus, the spontaneous emission spectrum is given by

$$\begin{aligned} S(\omega_k) &= \frac{\gamma_a}{2\pi} |\overline{A}[i(\omega_{ag} - \omega_k)]|^2 + \frac{\gamma_b}{2\pi} |\overline{B}[i(\omega_{bg} - \omega_k)]|^2 \\ &+ \frac{\gamma_c}{2\pi} |\overline{C}[i(\omega_{cg} - \Delta_c - \omega_k)]|^2 \\ &+ \frac{\gamma_d}{2\pi} |\overline{D}[i(\omega_{dg} - \Delta_d - \omega_k)]|^2 \quad (45) \end{aligned}$$

with  $\overline{A}(s)$ ,  $\overline{B}(s)$ ,  $\overline{C}(s)$ , and  $\overline{D}(s)$  given by Eqs. (38) and (39).

In Fig. 4, the spontaneous emission spectra of the system are plotted with different initial conditions: (a)  $A(0) = 1$  and  $B(0) = C(0) = D(0) = 0$ ; (b)  $B(0) = 1$  and  $A(0) = C(0) = D(0) = 0$ . In Fig. 4 (a), we assume that the system is prepared in level  $|a\rangle$  initially, and the black solid curves are for phase  $\Phi = \pi/2$  and the red dashed curves for  $\Phi = -\pi/2$ . When  $\Phi = -\pi/2$ , as the population can transfer from the level  $|a\rangle$  to level  $|b\rangle$ , so there is a peak around the resonant frequency  $\omega_{bg}$  in the spontaneous emission spectra. Instead, there is almost no population transferring from the level  $|a\rangle$  to level  $|b\rangle$  when  $\Phi = \pi/2$ , so that the peak around the frequency  $\omega_{bg}$  is eliminated. In Fig. 4 (b), we assume that the system is prepared in level  $|b\rangle$  initially. When  $\Phi = \pi/2$ , as the

population can transfer from the level  $|b\rangle$  to level  $|a\rangle$ , so there is a peak around the resonant frequency  $\omega_{ag}$  in the spontaneous emission spectra. Instead, there is almost no population transferring from the level  $|b\rangle$  to level  $|a\rangle$  when  $\Phi = -\pi/2$ , so that the peak around the frequency  $\omega_{ag}$  is eliminated.

In addition, the dependence of the the spontaneous emission spectra  $S(\omega_k = \omega_{ag})$  and  $S(\omega_k = \omega_{bg})$  on the synthetic magnetic flux  $\Phi$  are shown in Fig. 5, with the system initially prepared in level  $|b\rangle$  and  $|a\rangle$  respectively. We have  $S(\omega_k = \omega_{ag}) > S(\omega_k = \omega_{bg})$  for synthetic magnetic flux  $0 < \Phi < \pi$ , which corresponds with  $T_{ba}(t) < T_{ab}(t)$  in Fig. 3(a); in the contrast, we have  $S(\omega_k = \omega_{ag}) < S(\omega_k = \omega_{bg})$  for synthetic magnetic flux  $-\pi < \Phi < 0$ , conforming to  $T_{ba}(t) > T_{ab}(t)$ . Thus we can also observe the nonreciprocal transitions by contrasting the difference of the spontaneous emission spectra  $S(\omega_k = \omega_{ag})$  and  $S(\omega_k = \omega_{bg})$  with the system prepared in level  $|b\rangle$  or  $|a\rangle$  initially.

## V. CONCLUSIONS

A theoretically scheme was proposed to realize nonreciprocal transition between two indirectly coupled en-

ergy levels in a multi-level atomic system with cyclic four-level transition. The spontaneous emission spectra of the multi-level system with nonreciprocal transition was also investigated, and the nonreciprocal transition results in the elimination of a spectral line in the spontaneous emission spectrum, which can be used to measure the nonreciprocal transition experimentally. The scheme in this paper can be applied for observing nonreciprocal transition in the natural atoms with parity symmetry, which will broaden the application sphere of nonreciprocal transition.

## Acknowledgement

X.-W.X. and H.-Q.S. are supported by the National Natural Science Foundation of China (NSFC) under Grant No. 12064010, and the Natural Science Foundation of Jiangxi Province of China under Grant No. 20192ACB21002. A.-X.C. is supported by NSFC under Grant No. 11775190.

- 
- [1] R. K. Pathria, *Statistical Mechanics*, 2nd ed. (Butterworth-Heinemann, Oxford, 1996).
- [2] A. Einstein, On the quantum theory of radiation, *Phys. Z.* **18**, 121 (1917).
- [3] P. Král and M. Shapiro, Cyclic Population Transfer in Quantum Systems with Broken Symmetry, *Phys. Rev. Lett.* **87**, 183002 (2001).
- [4] H. Li, V. A. Sautenkov, Y. V. Rostovtsev, G. R. Welch, P. R. Hemmer, and M. O. Scully, Electromagnetically induced transparency controlled by a microwave field, *Phys. Rev. A* **80**, 023820 (2009).
- [5] W. Z. Jia and L. F. Wei, Gains without inversion in quantum systems with broken parities, *Phys. Rev. A* **82**, 013808 (2010).
- [6] Y. X. Liu, J. Q. You, L. F. Wei, C. P. Sun, and F. Nori, Optical Selection Rules and Phase-Dependent Adiabatic State Control in a Superconducting Quantum Circuit, *Phys. Rev. Lett.* **95**, 087001 (2005).
- [7] J. E. Mooij, T. P. Orlando, L. Levitov, L. Tian, C. H. van der Wal, and S. Lloyd, Josephson persistent-current qubit, *Science* **285**, 1036 (1999).
- [8] P. Král, I. Thanopoulos, M. Shapiro, and D. Cohen, Two-Step Enantio-Selective Optical Switch, *Phys. Rev. Lett.* **90**, 033001 (2003).
- [9] Y. Li, C. Bruder, and C. P. Sun, Generalized Stern-Gerlach Effect for Chiral Molecules, *Phys. Rev. Lett.* **99**, 130403 (2007).
- [10] L. Zhou, L. P. Yang, Y. Li, and C. P. Sun, Quantum Routing of Single Photons with a Cyclic Three-Level System, *Phys. Rev. Lett.* **111**, 103604 (2013).
- [11] Z. H. Wang, C. P. Sun, and Y. Li, Microwave degenerate parametric down-conversion with a single cyclic three-level system in a circuit-QED setup, *Phys. Rev. A* **91**, 043801 (2015).
- [12] Y. X. Liu, H. C. Sun, Z. H. Peng, A. Miranowicz, J. S. Tsai, and F. Nori, Controllable microwave three-wavemixing via a single three-level superconducting quantum circuit, *Sci. Rep.* **4**, 7289 (2014).
- [13] Y. J. Zhao, J. H. Ding, Z. H. Peng, Y. X. Liu, Realization of microwave amplification, attenuation, and frequency conversion using a single three-level superconducting quantum circuit, *Phys. Rev. A* **95**, 043806 (2017).
- [14] A. Barfuss, J. Kölbl, L. Thiel, J. Teissier, M. Kasperczyk, and P. Maletinsky, Phase-controlled coherent dynamics of a single spin under closed-contour interaction, *Nature Phys.* **14**, 1087 (2018).
- [15] X. W. Xu, Y. J. Zhao, H. Wang, A. X. Chen, and Y. X. Liu, Nonreciprocal transition between two nondegenerate energy levels, arXiv:1908.08323 [quant-ph].
- [16] X. W. Xu, C. Ye, Y. Li, A. X. Chen, Enantiomeric-excess determination based on nonreciprocal-transition-induced spectral-line elimination, *Phys. Rev. A* **102**, 033727 (2020).
- [17] J. Zhang, B. Peng, S. K. Özdemir, Y. X. Liu, H. Jing, X. Y. Lü, Y. L. Liu, L. Yang, and F. Nori, Giant nonlinearity via breaking parity-time symmetry: A route to low-threshold phonon diodes, *Phys. Rev. B* **92**, 115407 (2015).
- [18] Y. Jiang, S. Maayani, T. Carmon, F. Nori, and H. Jing, Nonreciprocal phonon laser, *Phys. Rev. Appl.* **10**, 064037 (2018).
- [19] S. Y. Zhu, R. C. F. Chan, and C. P. Lee, Spontaneous emission from a three-level atom, *Phys. Rev. A* **52**, 710

- (1995).
- [20] S. Y. Zhu and M. O. Scully, Spectral Line Elimination and Spontaneous Emission Cancellation via Quantum Interference, *Phys. Rev. Lett.* **76**, 388 (1996).
- [21] V. Weisskopf and E. Wigner, Berechnung der natürlichen Linienbreite auf Grund der Diracschen Lichttheorie. *Z. Physik* **63**, 54 (1930).
- [22] M. O. Scully and M. S. Zubairy, *Quantum Optics*, Cambridge University Press, Cambridge, England (1997).